Numerical analysis in biofluid dynamics: eye, nose and blood vessels

Jan O. Pralits

Department of Civil, Chemical and Environmental Engineering
University of Genoa, Italy
jan.pralits@unige.it

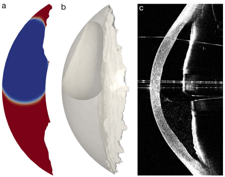

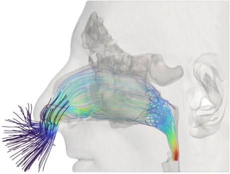

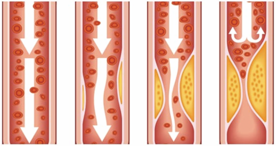

Assessing virtual surgeries of the human nose via computational fluid dynamics

E. Segalerba[1], M. Quadrio[2], J. O. Pralits[1]

[1] Department of Civil, Chemical and Environmental Engineering, University of Genoa, Italy,
[2] Department of Aerospace Science and Technologies, Politecnico di Milano, Milano, Italy

Anatomy and functioning

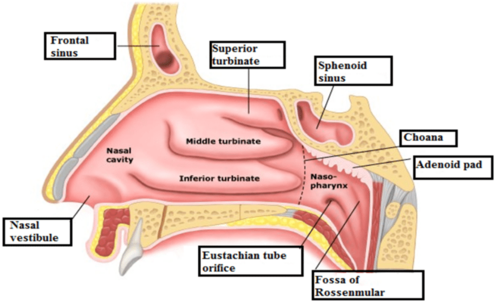

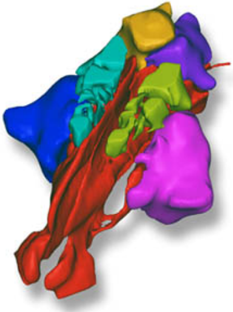

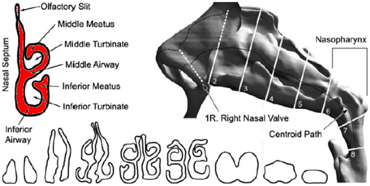

It the nose flow important?

- At least 1/3 of the adult world population is troubled with nasal breathing difficulties[1]
- In 2014, the one-year (only!) cost of cronic rhinosinusits (alone!) in US (only!) was $22bn[2]
- Certain nose surgeries have 50% failure rate[3]

Very large margin for improvement

[1]Stewart et al. Int J Gen Med 2010
[2]Smith et al. The Laryngoscope 2015
[3]Sundh & Sonnergreen, Eur Arch Otholaringol 2015

The workflow

1. Segment the CT scan
2. Construct a volume mesh
3. Compute the CFD solution (DNS, LES, RANS, ...)

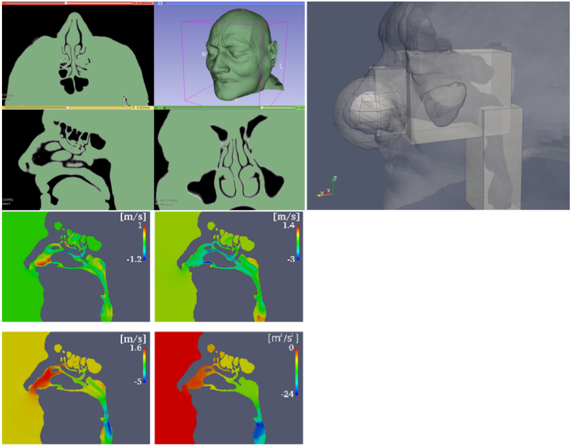

The workflow

1. Segment the CT scan
2. Construct a volume mesh
3. Compute the CFD solution (DNS, LES, RANS, ...)

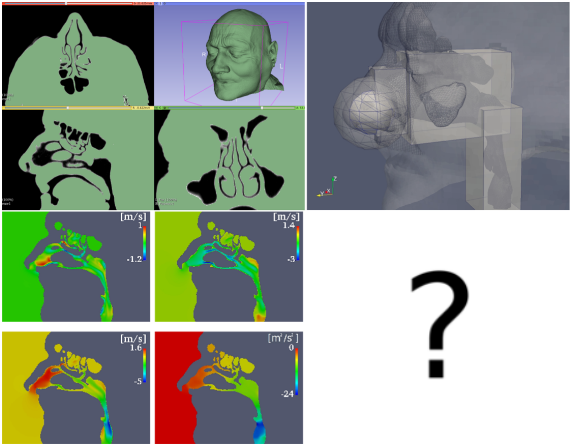

How to proceed?

Bringing CFD into the **clinical** setting requires:

- Assess **reliability** through a solid benchmark
- **Extract CFD-derived information** that is useful to surgeons

The benchmark

Reliability

- An unique Reynolds number does not exist
- Most authors use RANS, but the flow is not turbulent
- Most authors use steady RANS, but the flow is low-Re and unsteady
- Geometry created from CT scan not unique

Ongoing

- tomo-PIV experiment being developed at OTH Regensburg
- An ad-hoc DNS solver has been developed at Polimi (IMB, fast)

How to extract useful information

The lack of the functionally normal nose

CFD solution alone does not help surgeons to find the best surgery

- Main reason: **lack of functionally normal reference nose**
- Shape optimization, but an **objective function is lacking** (well-being?)
- Strong inter-subject anatomical **variations** with different functional significance
- How do we **compare** 2 anatomies? Ex. pre-op and post-op

How to compare 2 anatomies

Purpose

- Compare pre-op and post-op, HOW?
- Compare 2 healthy anatomies, HOW?
- Neglected in the literature
- **Goal**: show that comparison criterion affects the results

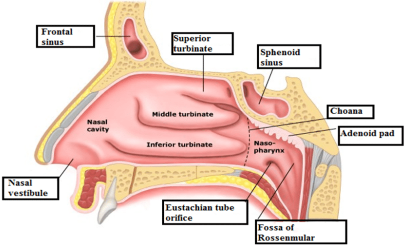

How to compare 2 anatomies

Method

- Compare pre-op and post-op
- Endoscopic Medial Maxillectomy (EMM)

3 conditions:

- CPG (Δp)
- CFR ($\dot{Q}$)
- CPI (Power$=\dot{Q}\Delta p$)

Flow model:

- Large Eddy Simulation (LES)
- Mesh: $\approx$ 15 million cells
- 1.5 seconds (768 processors, 24 hours)

pre-op **post-op**

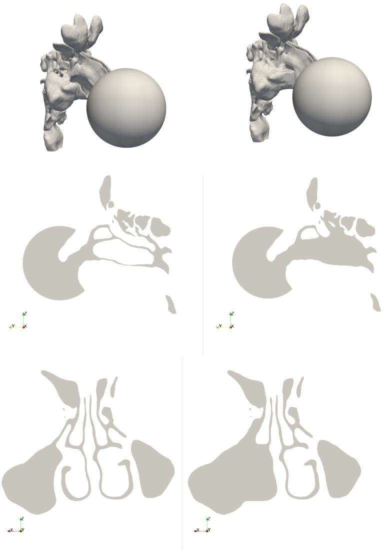

How to compare 2 anatomies

Results: pre-op

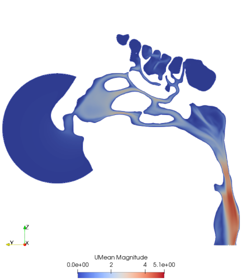

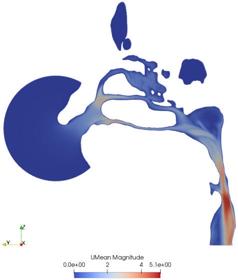

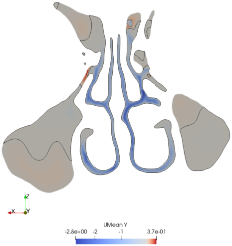

same results in all cases: CPG, CFR CPI

How to compare 2 anatomies

Results: post-op, difference between CPG and CFR

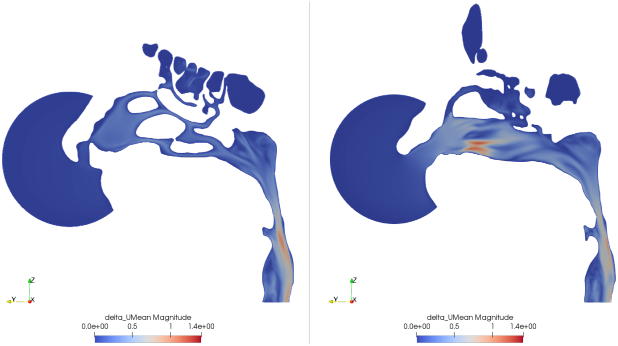

VERY large localized differences

How to compare 2 anatomies

Results: comparing global values

flow forcing	CPG		CFR		CPI	
cases	pre-op	post-op	pre-op	postop	pre-op	post-op
$\dot{Q} \times 10^4\ [m^3/s]$	2.67	3.12	2.67	2.67	2.67	2.95
$p_{thr}\ [Pa]$	-24.45	-24.45	-24.52	-18.50	-24.45	-22.14
$Power \times 10^3\ [W]$	-6.53	-7.63	-6.55	-4.94	-6.53	-6.53
variation in [%]	$\Delta\dot{Q} = 16.9\%$ $\Delta p_{thr} = 0\%$ $\Delta Power = 16.9\%$		$\Delta\dot{Q} = 0\%$ $\Delta p_{thr} = -24.6\%$ $\Delta Power = -24.6\%$		$\Delta\dot{Q} = 10.5\%$ $\Delta p_{thr} = -9.5\%$ $\Delta Power = 0\%$	

VERY large differences in GLOBAL quantities

How to compare 2 anatomies

Conclusions

- The flow forcing choice is crucial
- Large differences in **GLOBAL** quantities
- Large differences in **LOCAL** quantities
- Worst choice is **CPG** (geometry dependent)
- CPI or CFR? **consensus among clinicians** is still to be established.

OpenNOSE community

- Active since 2011, Website (www.open-nose.org) launch 2023
- Multi-disciplinary ($\approx$30 people), Polimi leader
- Driven by clinical problems and ENT surgeons
- Aim: develop virtual surgery, support to surgeons
- DNS, experimental data, anatomy data will be freely available

Acknowledgement to the OpenNOSE gang

Anatomy and functioning of the eye

Anterior chamber flow

- production/drainage
- myosis/mydriasis
- buoyancy-driven
- saccades

Vitreous chamber flow

- sub-retinal
- saccades

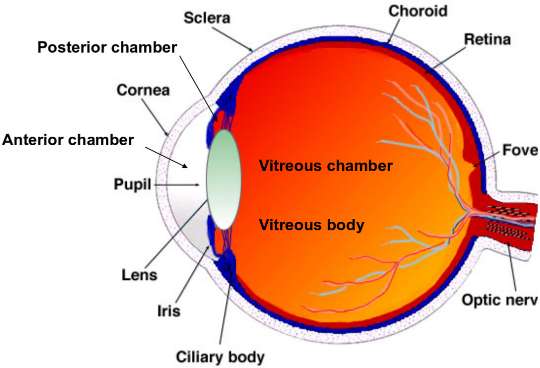

Retinal detachment

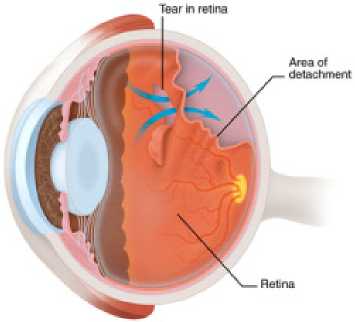

Posterior vitreous detachment (PVD)

- more common in myopic eyes;
- preceded by changes in vitreous macromolecular structure reasons.
- If the retina detaches $\rightarrow$ loss of vision;

Rhegmatogeneous retinal detachment:

- fluid enters through a retinal break into the sub retinal space and peels off the retina.

Risk factors:

- **myopia;**
- posterior vitreous detachment (PVD);
- lattice degeneration;
- ...

Investigations

Computer modeling of Rhegmatogenous Retinal Detachment

D. Natali[1], S. Kheirandish[1], R. Repetto[1], J. O. Pralits[1],
J. H. Siggers[2], Tom H. Williamson[3], M. Romano[4]

[1] Department of Civil, Chemical and Environmental Engineering, University of Genoa, Italy,
[2] Department of Bioengineering, Imperial College London, London SW7 2AZ, UK,
[3] Retina Surgery, 50-52 New Cavendish Street, London W1G 8TL, UK,
[4] Department of Biomedical Sciences, Humanitas University, Milan, Italy

Published:
Journal of Fluids and Structures, 2018; 82:245–257
Journal of Fluids and Structures, 2022; 115:103766

Purpose

- **1 in 10,000** of the population
- Caused by retinal **breaks in the peripheral retina**
- Unchecked RRD is a **blinding condition**
- Postulated that **saccadic eye movements** create liquefied vitreous flow in the eye, which help to lift the retina
- Experience says that the **hole** condition detaches quicker than the **free flap** condition
- **Objective**: investigate if **hole** or **free flap** has larger tendency to detach

Method I

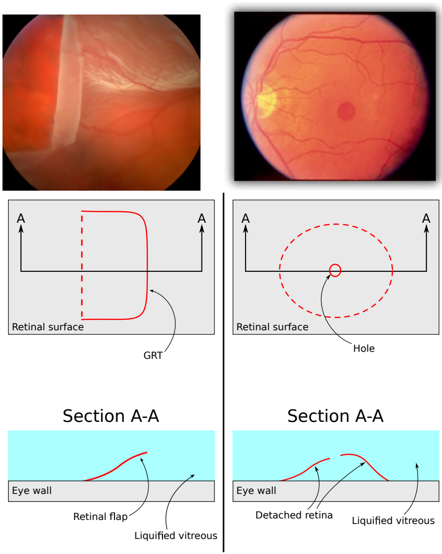
A
A
Retinal surface
GRT
A
A
Retinal surface
Hole
Section A-A
Eye wall
Retinal flap
Liquified vitreous
Section A-A
Eye wall
Detached retina
Liquified vitreous

Method II

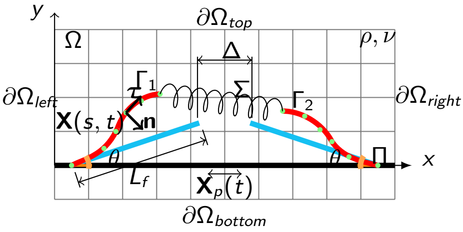

Fluid flow

$$\begin{cases} \dfrac{\partial \mathbf{u}}{\partial t} + \mathbf{u} \cdot \nabla \mathbf{u} = -\nabla p + \dfrac{1}{Re} \nabla^2 \mathbf{u} + \mathbf{f} \\ \nabla \cdot \mathbf{u} = 0 \end{cases},$$

For the slender 1D structure

$$\frac{\partial^2 \mathbf{X}}{\partial t^2} = \frac{\partial}{\partial s}\left(T \frac{\partial \mathbf{X}}{\partial s}\right) - \frac{\partial^2}{\partial s^2}\left(\gamma \frac{\partial^2 \mathbf{X}}{\partial s^2}\right) + Fr \mathbf{g} - \mathbf{F}$$

Method III

Wall motion (Repetto et al. (2005)), angles tested 8°, 15°, duration 0.045 s

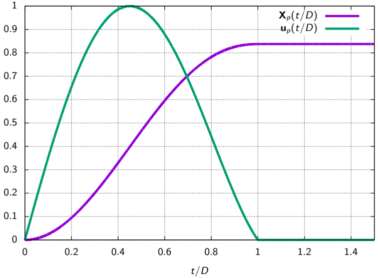

All data from the literature

- Retinal thickness 70 μ
- Youngs modulus from measurements
- Liquid similar to water
- **Varying**: L, θ and Δ

Dynamics for retinal tear

L=2 mm, $\theta = 33.6^\circ$

Movie 1

Dynamics for retinal hole

L=2 mm, $\theta = 33.6^\circ$, $\Delta = 0.17$ mm

Movie 2

Winkler theory

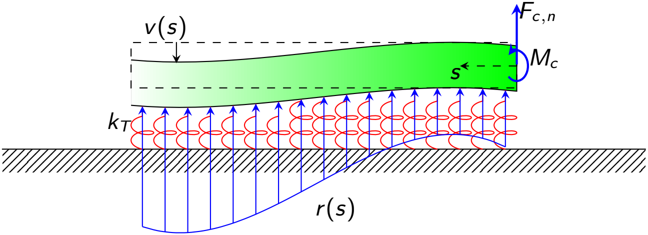

$$d = \max(v|_{s=0}, 0) = \max\left(\frac{\alpha M_c + F_{c,n}}{2\alpha^3\gamma}, 0\right),$$

where α is the ratio between the soil spring rigidity k_T and foundation beam stiffness γ.

d is the tendency to detach

Different filament lengths L^*: maximum tendency to detach

clamping angle $\theta = 33.56^\circ$, $\Delta^* = 0.17mm$ (retinal hole)

15 degree saccade, **8 degree saccade**

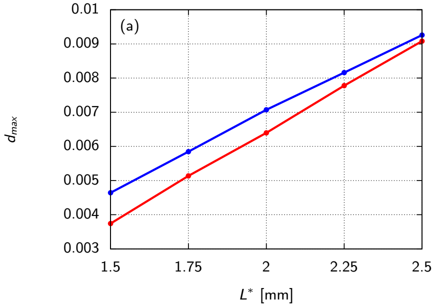

Tear

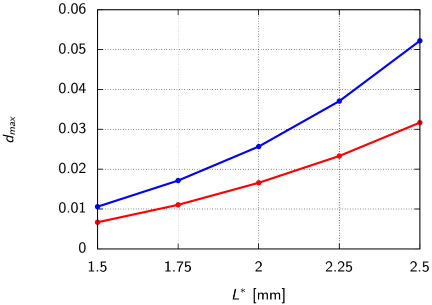

Hole

Increasing L^* increases the maximum value of $d_{0,max}$

Different clamping angles θ: maximum tendency to detach

length $L^* = 2$ mm, $\Delta^* = 0.17mm$ (retinal hole)
15 degree saccade, **8 degree saccade**

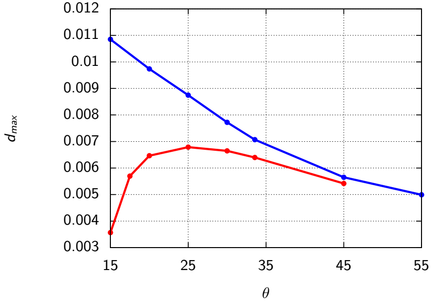

Tear

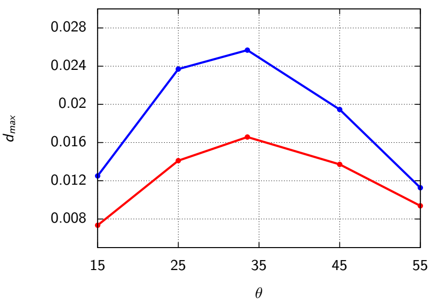

Hole

A maximum value of d_{max} is found

Comparison horseshoe tear & hole: maximum tendency to detach

clamping angle $\theta = 33.56^\circ$, $\Delta^* = 0.17mm$ (retinal hole)

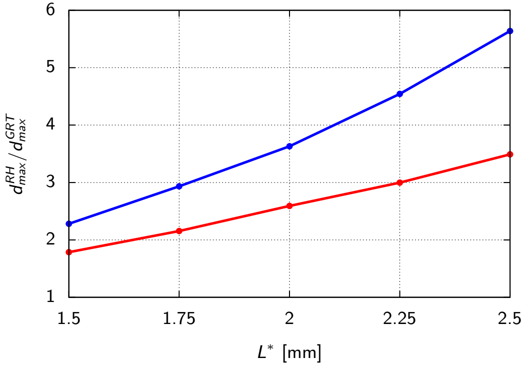

The retinal hole is more prone to detach compared to horseshoe tear

Conclusions

The main results, for GRT and RH using realistic parameter values, show:

- **Increasing** L^* increases the tendency to detach (both GRT & RH).

Collaborations with a **surgeon confirms** that these results are in line with their findings and will give **useful guidelines** for treatment of retinal breaks.

Conclusions

The main results, for GRT and RH using realistic parameter values, show:

- **Increasing** L^* increases the tendency to detach (both GRT & RH).
- **Changing** θ, the maximum tendency to detach is found for; GRT at a clamping angle of $\approx 25^\circ$ (8 degrees saccade) and $\approx 35^\circ$ for RH, independently of the saccadic amplitude.

Collaborations with a **surgeon confirms** that these results are in line with their findings and will give **useful guidelines** for treatment of retinal breaks.

Conclusions

The main results, for GRT and RH using realistic parameter values, show:

- **Increasing** L^* increases the tendency to detach (both GRT & RH).
- **Changing** θ, the maximum tendency to detach is found for; GRT at a clamping angle of $\approx 25^\circ$ (8 degrees saccade) and $\approx 35^\circ$ for RH, independently of the saccadic amplitude.
- **Changing** Δ^*, the hole size, has little effect on the tendency to detach for both saccades tested.

Collaborations with a **surgeon confirms** that these results are in line with their findings and will give **useful guidelines** for treatment of retinal breaks.

Conclusions

The main results, for GRT and RH using realistic parameter values, show:

- **Increasing** L^* increases the tendency to detach (both GRT & RH).
- **Changing** θ, the maximum tendency to detach is found for; GRT at a clamping angle of $\approx 25^\circ$ (8 degrees saccade) and $\approx 35^\circ$ for RH, independently of the saccadic amplitude.
- **Changing** Δ^*, the hole size, has little effect on the tendency to detach for both saccades tested.
- **RH vs GRT**, the tendency to detach of a RH, compared to a GRT, is 2-3.5 times larger for retinal flaps of 1.5-2.5 mm, and the ratio increases for longer flap lengths. This ratio increases as the saccadic amplitude is increased.

Collaborations with a **surgeon confirms** that these results are in line with their findings and will give **useful guidelines** for treatment of retinal breaks.

Optimization of patient positioning for improved healing after corneal transplantation

M. Alberti[1], J. Cabrerizo[1,2], V. Garcia Bennett[3], M. Quadrio[3], J. O. Pralits[4]

[1] Department of Ophthalmology, Rigshospitalet, Glostrup, Denmark
[2] Copenhagen Eye Foundation, Copenhagen, Denmark
[3] Department of Aerospace Science and Technologies, Politecnico di Milano, Milano, Italy
[4] Department of Civil, Chemical and Environmental Engineering, University of Genoa, Italy

Published:
Translational Vision Science & Technology, 2019; 8(6):9
Submitted:
Journal of Biomechanics, 2022

Purpose I

Corneal endothelial cell dysfunctions

- Fuchs' endothelial dystrophy (up to 11% of US population above 40 years)
- Congenital hereditary endothelial dystrophy
- Corneal edema due to complications from other types of eye surgery

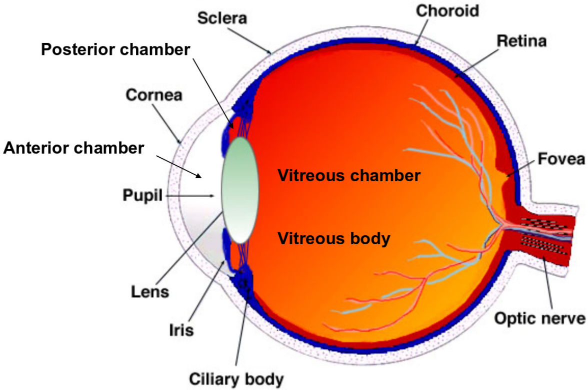

Purpose II

DMEK procedure (about 15 minutes)

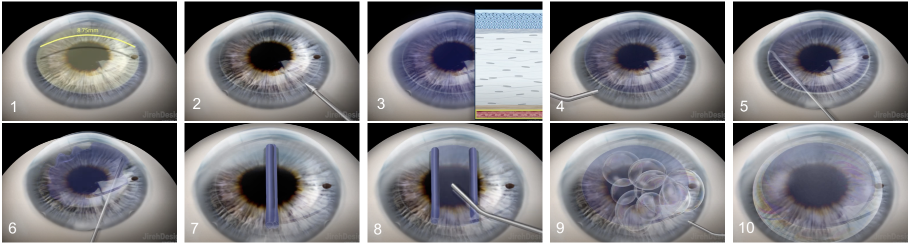

Post-operative problem

- graft peal off, mostly in lower quadrant ($>$ 20% of cases)

Objective

- Analyse optimal patient positioning for improved healing

Method I

Compute stationary solution of air bubble in aqueous humor ($\approx$ water) solving

- incompressible Navier-Stokes equations...
- coupled with transport equation for phase fraction γ (VOF)

$$\nabla \cdot U = 0,$$

$$\rho \frac{\partial U}{\partial t} + \rho U \cdot \nabla U - \mu \nabla^2 U = -\nabla p_d - \rho g \cdot x + \sigma \kappa \nabla \gamma,$$

$$\frac{\partial \gamma}{\partial t} + \nabla \cdot (U\gamma) + \nabla \cdot [U_r (1 - \gamma)] = 0,$$

Important parameters

- anterior chamber shape
- surface tension
- static contact angles (our measurements)
- densities
- gravitational acceleration

LESS Important parameters

- viscosities

Method II

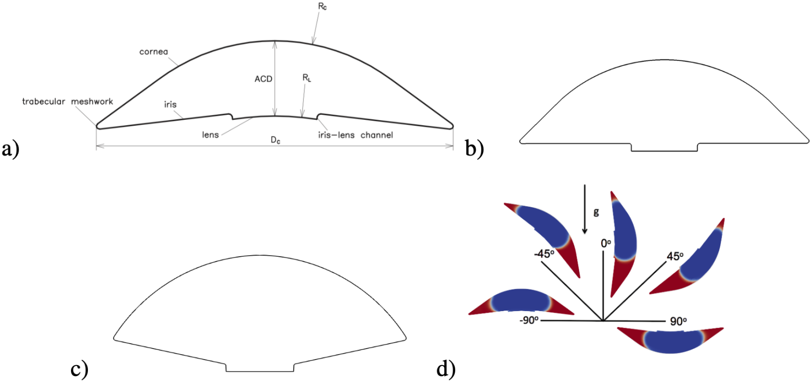

Parametric study

- ACD
- with and without natural lens
- gas fill (**time**)
- patient position

Method III

Measurements

- gas-graft coverage in %
- gas exposure on graft over time

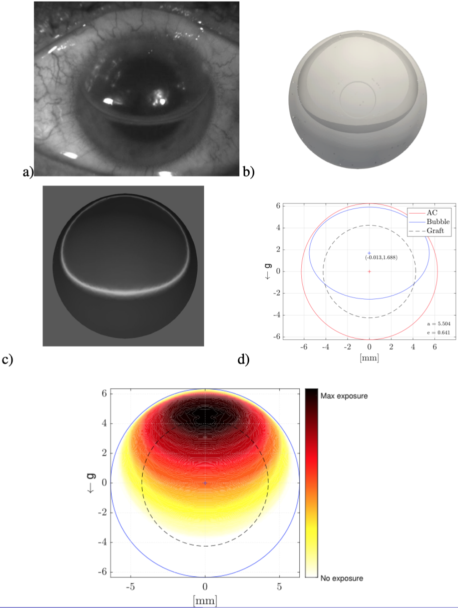

Results I

Gas-graft coverage

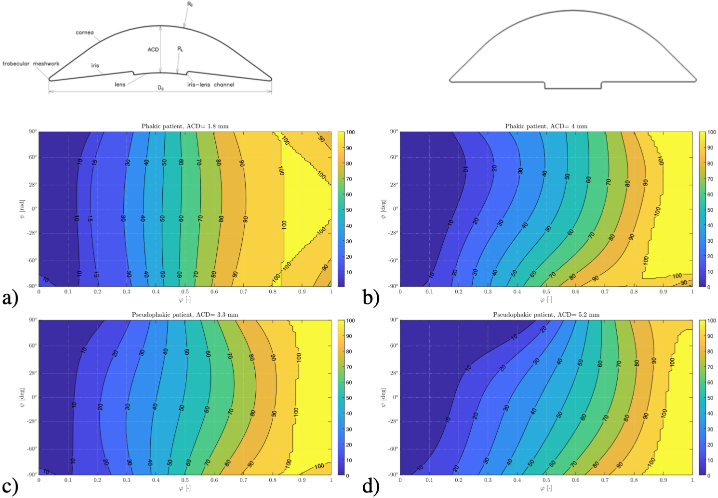

Results II

Patient position that **maximises** gas-graft coverage

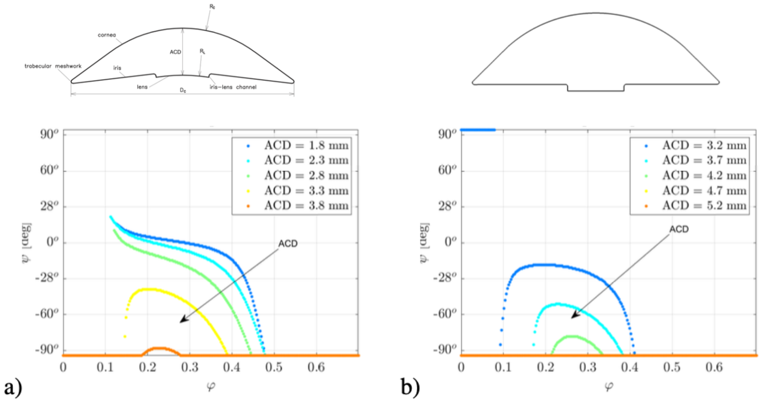

Results III

Mean graft coverage **changing patient position over time**

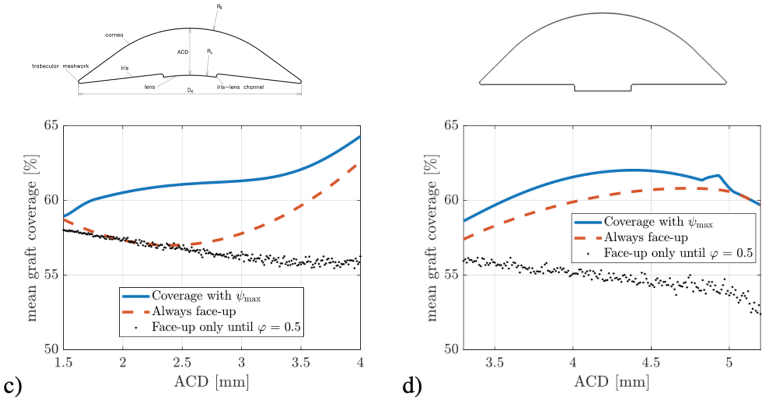

Results IV

Gas exposure on graft over time: **Optimal versus Random patient positioning**

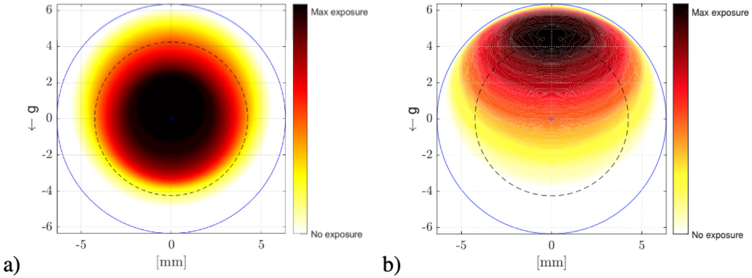

Conclusions

- Patient positioning is **negligible** if ACD is small
- Optimal patient positioning important **only** for larger ACD
- Exposure (position of gas bubble) more sensitive than Coverage (%) w.r.t. patient positioning

Engineered small-diameter vascular prostheses: a study in bioreactor

P.F. Ferrari[1,3], G. De Negri Atanasio[1], J.O. Pralits[1,3], D. Palombo[2,3] & P. Perego[1,3]

[1] Department of Civil, Chemical and Environmental Engineering, University of Genoa, Italy,
[2] Dipartimento di scienze chirurgiche e diagnostiche integrate - DISC, University of Genoa, Italy
[3] Centro Interdipartimentale BELONG, Research Centre of Biologically Inspired Engineering in Vascular Medicine and Longevity, University of Genoa, Italy

Submitted:
Journal of Biomedical Materials Research Part A, 2022

Motivation

- Current strategies for aterosclerosi is substitute with bioprotesi
- Available protesi are $D > 7$mm (eg. Dacron)
- **Goal**: produce engineered bioprotesi $D < 6$mm

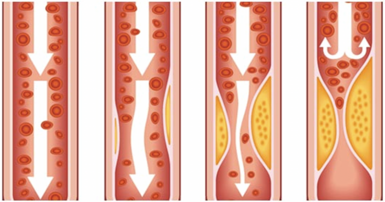

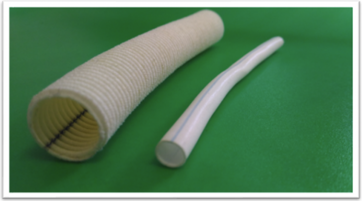

Method I

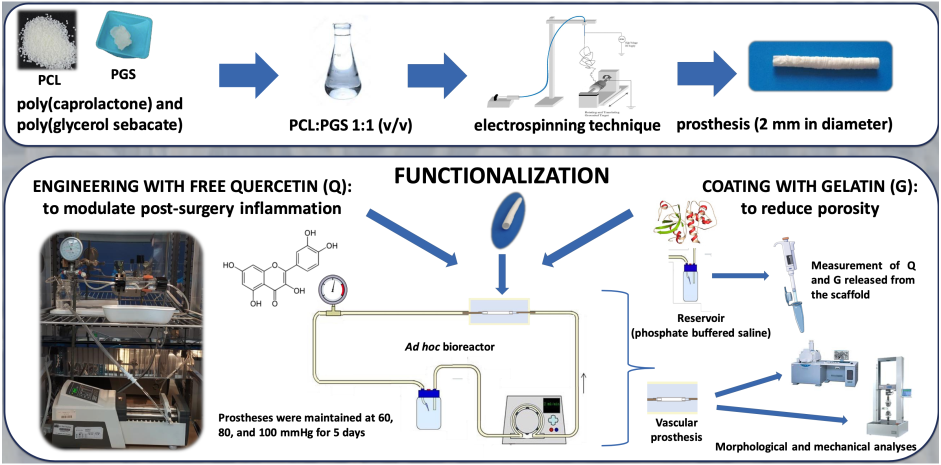
PCL
PGS
poly(caprolactone) and poly(glycerol sebacate)
PCL:PGS 1:1 (v/v)
electrospinning technique
prosthesis (2 mm in diameter)
FUNCTIONALIZATION
ENGINEERING WITH FREE QUERCETIN (Q): to modulate post-surgery inflammation
COATING WITH GELATIN (G): to reduce porosity
HO
OH
O
Ad hoc bioreactor
Prostheses were maintained at 60, 80, and 100 mmHg for 5 days
Reservoir (phosphate buffered saline)
Measurement of Q and G released from the scaffold
Vascular prosthesis
Morphological and mechanical analyses

Method II

Modelling of fluid dynamics

- Predictive tool: experiments are long and costly
- Detailed results difficult to obtain experimentally
- Step-by-step:
  1. Newtonian steady state
  2. Newtonian unsteady (heart beat)
  3. Non-newtonian (similar to blood) unsteady

Method III

Newtonian steady state

- Incompressible flow
- Pipe geometry with smooth walls
- Steady state

Solution is analytical

$$\tau_W = -\mu \frac{8U}{D}$$

Results I

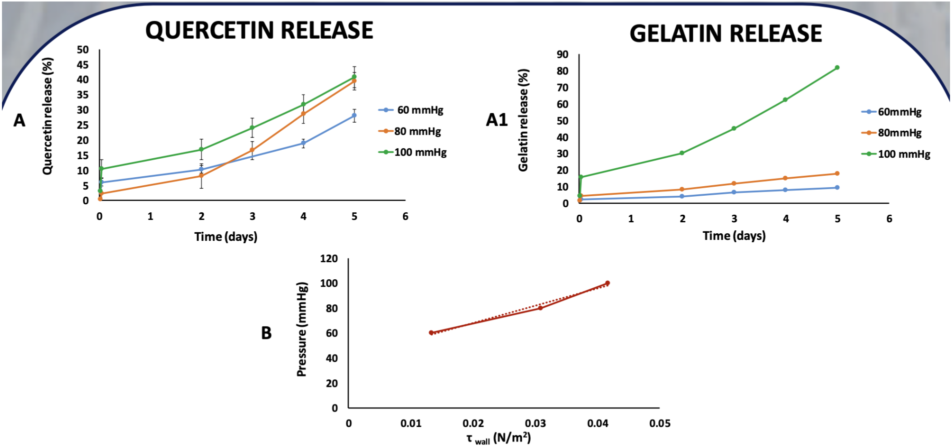
QUERCETIN RELEASE
A
Quercetin release (%)
Time (days)
60 mmHg
80 mmHg
100 mmHg
GELATIN RELEASE
A1
Gelatin release (%)
Time (days)
60mmHg
80mmHg
100 mmHg
B
Pressure (mmHg)
τ wall (N/m²)

Results II

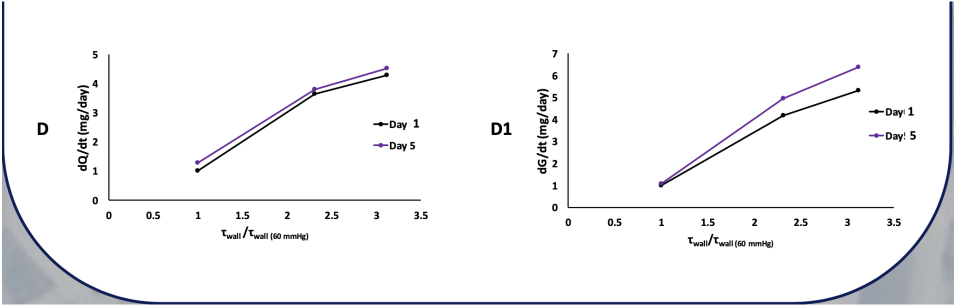
D
dQ/dt (mg/day)
5
4
3
2
1
0
0
0.5
1
1.5
2
2.5
3
3.5
τwall/τwall (60 mmHg)
Day 1
Day 5
D1
dG/dt (mg/day)
7
6
5
4
3
2
1
0
0
0.5
1
1.5
2
2.5
3
3.5
τwall/τwall (60 mmHg)
Day 1
Day 5

Ongoing

Newtonian unsteady

- Incompressible flow
- Pipe geometry with smooth walls
- Unsteady (signal from heart beat)

Solution is analytical

$$\tau_W = real \left\{ \sum_{n=1}^{N} P'_n \frac{R}{\Lambda_n} \frac{J_1(\Lambda_n)}{J_0(\Lambda_n)} e^{in\omega t} \right\}$$

where Λ_n depends on the Womersly number (non-dimensional frequency)

Movie 1

Movie 2

References I

B. Alamouti and J. Funk. Retinal thickness decreases with age: an oct study. *British Journal of Ophthalmology*, 87(7):899–901, 2003.

D. A. Atchison and G. Smith. *Optics of the human eye*. Butterworth-Heinemann, 2000.

D. A. Atchison, C. E. Jones, K. L. Schmid, N. Pritchard, J. M. Pope, W. E. Strugnell, and R. A. Riley. Eye shape in emmetropia and myopia. *Investigative Ophthalmology & Visual Science*, 45(10):3380–3386, 2004. doi: 10.1167/iovs.04-0292.

C. Bowd, R. N. Weinreb, B. Lee, A. Emdadi, and L. M. Zangwill. Optic disk topography after medical treatment to reduce intraocular pressure. *American Journal of Ophthalmology*, 130(3):280 – 286, 2000. ISSN 0002-9394. doi: http://dx.doi.org/10.1016/S0002-9394(00)00488-8. URL http://www.sciencedirect.com/science/article/pii/S0002939400004888.

M. Dogramaci and T. H. Williamson. Dynamics of epiretinal membrane removal off the retinal surface: a computer simulation project. *Br. J. Ophthalmol.*, 97 (9):1202–1207, 2013. doi: 10.1136/bjophthalmol-2013-303598.

C. R. Ethier, M. Johnson, and J. Ruberti. Ocular biomechanics and biotransport. *Annu. Rev. Biomed. Eng.*, 6:249–273, 2004.

References II

W. J. Foster, N. Dowla, S. Y. Joshi, and M. Nikolaou. The fluid mechanics of scleral buckling surgery for the repair of retinal detachment. *Graefe's Archive for Clinical and Experimental Ophthalmology*, 248(1):31–36, 2010.

I. L. Jones, M. Warner, and J. D. Stevens. Mathematical modelling of the elastic properties of retina: a determination of young's modulus. *Eye*, (6):556–559, 1992.

A. Reichenbach, W. Eberhardt, R. Scheibe, C. Deich, B. Seifert, W. Reichelt, K. Dähnert, and M. Rödenbeck. Development of the rabbit retina. iv. tissue tensility and elasticity in dependence on topographic specializations. *Experimental Eye Research*, 53(2):241 – 251, 1991. ISSN 0014-4835. doi: http://dx.doi.org/10.1016/0014-4835(91)90080-X. URL http://www.sciencedirect.com/science/article/pii/001448359190080X.

R. Repetto, A. Stocchino, and C. Cafferata. Experimental investigation of vitreous humour motion within a human eye model. *Phys. Med. Biol.*, 50:4729–4743, 2005.

I. A. Sigal, J. G. Flanagan, and C. R. Ethier. Factors influencing optic nerve head biomechanics. *Investigative Ophthalmology & Visual Science*, 46(11):4189, 2005. doi: 10.1167/iovs.05-0541. URL +http://dx.doi.org/10.1167/iovs.05-0541.

G. Wollensak and S. Eberhard. Biomechanical characteristics of retina. *Retina*, (24): 967–970, 2004.